Int. J. Electrochem. Sci., 17 **(2022)** Article Number: 221125, doi: 10.20964/2022.11.34

International Journal of
ELECTROCHEMICAL
SCIENCE
www.electrochemsci.org

Fabrication of Polymer based on Carbon Nanotube Electrospun Nanofibers as Anode for high-Performance Li-ion Battery

Zhiyuan Liu[1,2,3]

[1] Key Laboratory of Environment-
Friendly Composite Materials of the State Ethnic Affairs Commission, Lanzhou, Gansu 730030, China
[2] Gansu Provincial Biomass Function Composites Engineering Research Center, Lanzhou, Gansu 7300 30, China
[3] Key Laboratory for Utility of Environment-
Friendly Composite Materials and Biomass in University of Gansu Province, School of Chemical Engi neering, Northwest Minzu University, Lanzhou, Gansu 730030, China
E-mail: 177081616@xbmu.edu.cn

Received: 2 August 2022 / *Accepted:* 7 September 2022 / *Published:* 10 October 2022

The current study was conducted to fabricate and investigate polymer-CNT electrospun nanofibers as an anode for high-performance Li-ion batteries. The polymer-CNT nanofiber surface had numerous nanopores, beads, and protrusions in the nanofiber matrix, which suggested the production of a large effective surface area, according to analysis of morphology and structure. Examining the electrochemical characteristics using CV and GCD cycles revealed that the polymer-CNT nanofiber electrode is highly reversible. It also demonstrated great rate capabilities and strong cycling stability, with a reversible capacity of 1105.2mAhg^{-1} at a current density of 0.05 Ag^{-1}. The polymer-CNT nanofiber electrode demonstrated a columbic efficiency of almost 100% and exhibited a steady and reversible capacity, according to the results. When compared to other published carbon-based electrodes for lithium-ion batteries, the electrochemical performance of polymer-CNT nanofiber electrodes was found to be superior or appropriate. As a result, the one-of-a-kind porous polymeric nanofibers can be used to improve the electrochemical performance of Li-ion batteries.

Keywords: Electrospinning; Nanofibers; CNTs; Polymer; Li-ion battery; Reversible capacity

1. INTRODUCTION

The fast development of electric cars over the past few decades has raised the demand for energy storage systems, which now must meet higher energy density, higher power density, and longer cycle life standards [1, 2]. Li-ion batteries have a variety of benefits over the other premium rechargeable battery technologies (nickel-cadmium or nickel-metal hydride). They have one of the

highest energy densities (100-265 Wh kg^{-1}) of any battery technology available today [3-5]. Lithium-ion has disadvantages despite overall benefits [6, 7]. Due to its inherent fragility and the need for a protective circuit to maintain safe operation, solid state charging experiences substantial volume variations and a slow charging rate [8, 9]. Due to their high energy density and long-term stability, flexible Li-ion batteries have attracted a lot of research because they can also be useful in practical applications like wearable electronic devices, roll-up displays, touch screens, conformable active radio-frequency identification tags, and wearable sensors [10, 11].

The mechanical aspects and deformation circumstances, such as bending, folding, twisting, and pressing, have not kept up with advancements in these flexible energy devices [12, 13]. The downside of using flexible Li-ion battery applications with typical Li-ion electrodes is the poor energy density and power capacity of graphite as a commercial anode material [14, 15]. Other commercial Li-ion batteries' active components, binders, and conductive additives are easily separable from the foils made of copper and aluminum that operate as current collectors [16, 17]. Studies showed that the supercapacitors' high power density and excellent cycling stability enable them to deliver quick electrostatic charge dispersion and accumulation [18, 19]. However, the physical adsorption/desorption mechanism and low cycle stabilities of supercapacitors limit their applicability [20-22]. As a result, additional research is needed to fabricate flexible Li-ion batteries with excellent cycling stability, energy, and power density employing hybrids, nanostructures, and nanocomposites as new electrode materials [23, 24]. The creation of flexible energy storage devices has been made possible by the use of carbon-based nanofibers and CNTs in polymer nanocomposites, one type of nanostructured material [25-29].

Polymer nanofibers are a consequential class of 1D nanomaterials. The diameter of nanofibers is often less than 100 nm. Currently, there are three techniques available for the synthesis of nanofibers: electrospinning, self-assembly, and phase separation [30]. Of these techniques, electrospinning is the most widely studied and has also demonstrated the most promising results in terms of tissue engineering applications [31]. Nanofibers have many possible technological and commercial applications. They are used in tissue engineering, drug delivery, seed coating material, cancer diagnosis, lithium-air batteries, optical sensors, air filtration, redox-flow batteries and composite materials. Synthetic polymer nanofibers are made from nylon, acrylic, polycarbonate, polysulfones, and fluropolymers, among other polymers [30, 31].

Hou and Reneker [32] reported the fabrication of hierarchical structure of CNTs on carbon nanofibers. They described an electrospinning process for the fabrication of carbon nanofibers using a PAN and Fe(Acc) mixture dissolved in dimethylformamide, as well as the stabilization and carbonization of PAN and the reduction of the Fe in a high-temperature furnace in a mixture of H and Ar, and hexane vapor was used as a carbon source for the formation of CNTs on carbon nanofibers. They only studied the hierarchical structures of CNTs on carbon nanofibers and did not study the electrochemical properties of the resultant structures. In this study, polymer-CNT nanofibers were accomplished by the electrospinning technique using CNTs, dimethylformamide, PVP, and PAN, followed by thermal treatment in nitrogen flow. The structural and electrochemical properties of the resulted polymer-CNT nanofiber structures were investigated as anode for high-performance Li-ion batteries.

2. EXPERIMENT

2.1. Fabrication of PN/CNTs

The production of polymer-CNT nanofibers was accomplished by the electrospinning technique [33]. Sigma-Aldrich CNTs were ultrasonically dispersed in a 99.8% concentration of N,N′-Dimethylformamide (DMF) solution for 60 minutes at 4°C. The aforementioned solution was then appropriately diluted with polyacrylonitrile (PAN; Sigma-Aldrich) and polyvinylpyrrolidone (PVP); the result was 65 wt.% CNTs and 35 wt.% polymer solution, which was then heated at 45 °C while being stirred magnetically for an entire night. A polypropylene syringe with a needle (0.45 mm inner diameter) that was attached to a programmed syringe was used to inject the homogeneous mixture into the syringe. 1.5 mL/h of flow was delivered, and 16 kV of voltage was applied to the syringe tip to prepare nanofibers (HV30). The aluminum foil collection was 10 cm away from the tip. The resulting polymeric nanofibers were formed into 20 mm-diameter discs and vacuum-dried for 12 hours at 45 °C. The thermal treatment was then carried out at a ramp rate of 5 °C/min for 60 minutes, held for 60 minutes, and increased to 750 °C at a ramp rate of 7 °C/min, held for 60 minutes, and completed under nitrogen flow. The items were then chilled until they reached room temperature. In the absence of CNTs, the same method was used to prepare polymer-CNT nanofibers.

2.2. Characterizations

The morphologies of the generated nanofibers were studied using a scanning electron microscope (SEM). The nanofibers' crystal structures were examined using X-ray diffraction spectrometry (XRD). All electrochemical experiments were carried out using coin cells of the 2032 type, which contained prepared nanofibers punched into circular discs. The Li-metal disc was used as the counter electrode and reference electrode while the 2032-type coin batteries served as the working electrode in an Ar-filled glove box (NICHWELL -1500u). The ethylene carbonate (EC, 99 percent, Sigma-Aldrich) and diethyl carbonate mixture were used to create the electrolyte, which contained 1 M $LiPF_6$ (99.99 percent, Sigma-Aldrich) (DEC, 99 percent , Sigma-Aldrich). The separators were made using the Celgard-2400 membrane by the Japanese company Hochsen Corporation. The electrochemical tests were conducted using a potentiostat/galvanostat/electrochemical workstation (CS350, Wuhan Corrtest Instruments Corp., Ltd., China) at room temperature utilizing cyclic voltammetry (CV) at a scan rate of 0.1 mV/s in the voltage range of 0.001–3.0 V (versus Li/Li^+). Additionally, measurements using electrochemical impedance spectroscopy (EIS) on an amplitude of 10 mV in the frequency range of 10-1 Hz to 105 Hz were carried out. On a land battery testing system (CT2001A, Wuhan, China), the galvanostatic charge/discharge tests (GCD), rate performance, and cycling stability were performed.

3. RESULTS AND DISCUSSION

3.1. Analyses of morphology and structure

Figures 1a and 1b, respectively, show SEM images of polymer and polymer-CNT nanofibers. Figure 1a shows a matrix of interconnected polymer nanofibers with an average diameter of 80 nm. Porous, smooth, and bead-free nanofibers make up this matrix. Similar very open porous structures with well-connected morphology and an average diameter of 120 nm can be seen in SEM images of polymer-CNT nanofibers. Polymer-CNT nanofibers are different from polymer nanofibers in that they have a greater diameter and are less homogenous overall. Additionally, the surface of the polymer-CNT nanofibers exhibits multiple nanopores, the production of beads, and protrusions in the matrix of the nanofibers. These photos show that polymer-CNT nanofibers have a significantly higher effective surface area and higher porosity than polymer nanofibers.

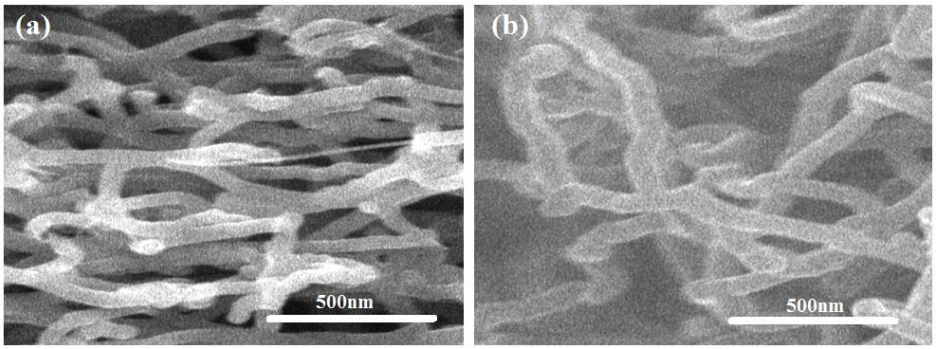

Figure 1. SEM images of (a) polymer nanofibers and (b) polymer-CNTs nanofibers.

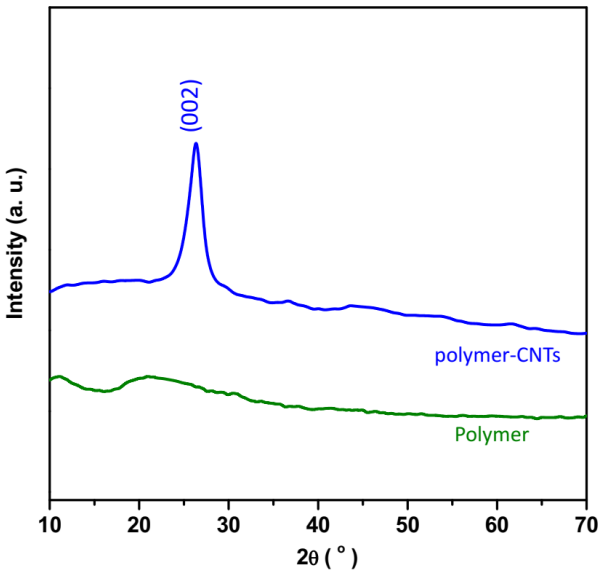

Figure 2. XRD patterns of polymer and polymer-CNTs nanofibers.

The XRD patterns of polymer and polymer-CNT nanofibers are shown in Figure 2. Due to the polymer's morphous structure and inadequate degree of crystallization, the XRD pattern of the polymer lacks any peaks [34, 35]. The (002) plane of the hexagonal graphitic structure of CNTs is shown by a distinct XRD peak at 2θ=25.98° in the XRD pattern of polymer-CNT nanofibers, as described in [36-38]. The SEM and XRD results show that the polymer-CNT nanofibers were successfully manufactured.

3.2. Study the electrochemical properties

The electrochemical performances of produced polymer and polymer-CNT nanofibers as anodes were investigated using CV and GCD cycle studies at ambient temperature in the voltage range of 0.001-3.0 V (versus Li/Li^+). Figures 3a and 3b show the CV curves for both anodes at 0.1 mV/s scan rate, which is indicative of typical CV curves for carbonaceous anode materials in Li-ion batteries [39, 40]. The reduction peak in the first cathodic scans can be attributed to solid electrolyte interphase (SEI) film formation [41, 42], co-insertion of the lithium ion into carbon, and irreversible interactions between the carbonaceous material and the electrolyte [43, 44]. A clear and steep peak that appears at about 0.11 V further supports the idea that lithium anions' rapid diffusion path was caused by their intercalation with the carbon framework [45-47]. The substantial overlap between the succeeding scans of the CV curves suggests that the polymer-CNT nanofiber electrode is extremely reversible and exhibits remarkable cycle stability [48, 49]. Additionally, the polymer-CNT nanofiber electrode's CV curve is rectangular in shape, indicating that capacitive processes [50, 51] are not present in the polymer electrode's CV curve.

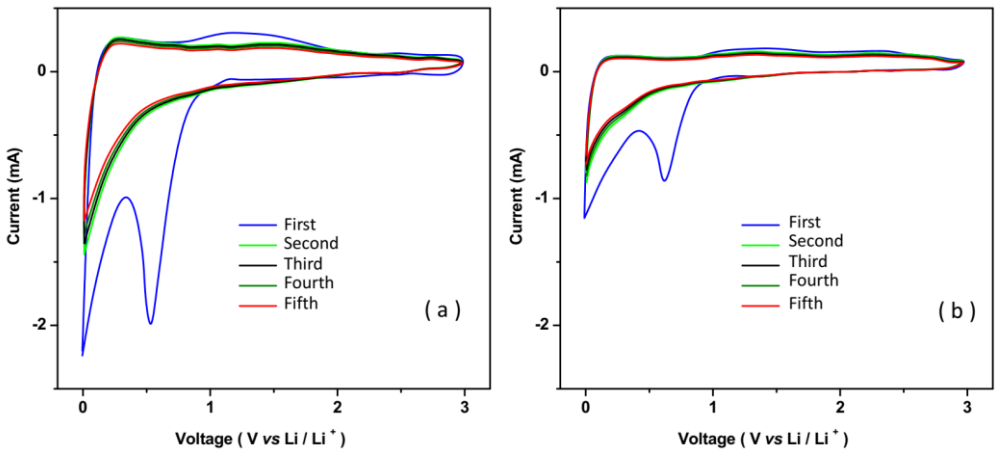

Figure 3. CV curves of prepared (a) polymer and (b) polymer-CNTs nanofibers at a scan rate of 0.1 mV/s in the voltage range of 0.001−3.0 V (vs Li/Li^+) at room temperature.

At a current density of 0.05 A g^{-1}, the GCD profiles of polymer and polymer-CNT nanofiber electrodes are shown in Figures 4a and 4b. The voltage capacity patterns of both electrodes are seen to be consistent with the CV findings. The irreversible peak in the CV curves and the irreversible peak of the initial scan are found to be compatible, and the charge profile of the polymer-CNT nanofibers

anode in the voltage window from 1.0 to 3.0 V is more flattish than that of the polymer nanofibers anode, demonstrating increased interfacial Li storage (a faradic capacitance on the surface) [52-54]. Li extraction from the polymer-CNT nanofiber sample's substantial electrochemically active surface area, microstructural flaws, pores, and functional groups on CNTs have all been linked to it [55-57]. Due to the interfacial Li storage, the polymer-CNT nanofiber electrode has greater initial reversible capacity retention (62.2%) than the polymer nanofiber electrode (55.8%). The total reversible capacity of polymer-CNT nanofibers in terms of Li storage by the interfacial reaction is supposed to increase with increasing interfacial area [58-60]. For effective capacity retention and the creation of an irreversible SEI layer on CNTs, the interfaces between the polymer nanofibers and the latter are crucial [61, 62]. Additionally, the initial discharge capacity of the polymer nanofiber electrode is 1616.3 mAh g^{-1} and the initial charge capacity is 939.8 mAh g^{-1}, while the initial discharge capacity of the polymer-CNTs nanofiber flexible electrode is higher at 2461.3 mAh g^{-1} and the initial charge capacity is 1488.32 mAh g^{-1}, which is about 4 times the theoretical capacity of graphite (372 mAh g^{-1}) [56, 63, 64]. It is important to note that both electrodes exhibit high irreversible capacity values, which are attributed to polymeric nanofibers. These fibers affect the contact resistance between the electrode surface and the SEI and improve the SEI's ability to adhere to the electrode surface, which can prevent electrolyte decomposition and result in the formation of thin, uniform, flexible, and subsequently advantageous SEI films [65-67]. The polymer-CNT nanofiber electrode is seen to demonstrate a columbic efficiency of around 100% during the first cycle, as well as a stable and reversible capacity. As a result, the one-of-a-kind porous polymeric nanofibers can be used to enhance the electrochemical performance of Li-ion batteries.

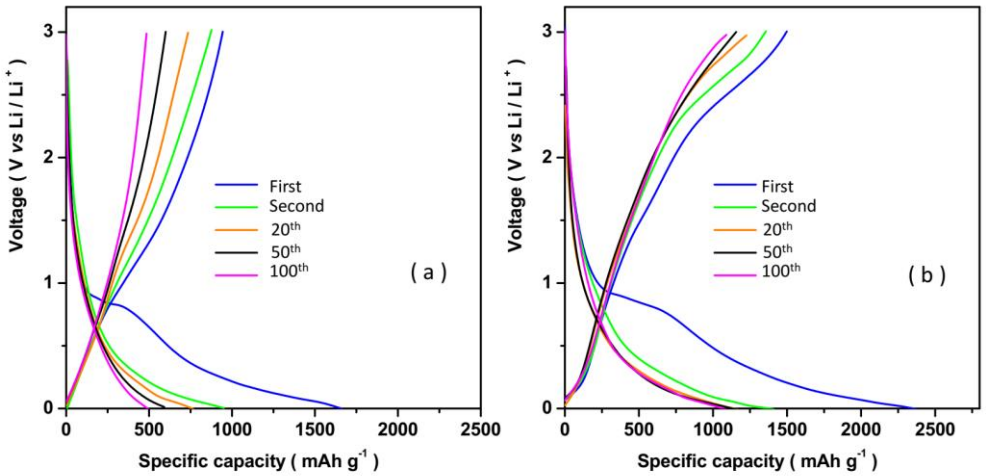

Figure 4. GCD voltage profiles of (a) polymer and (b) polymer-CNTs nanofibers electrode under current density of 0.05 A g^{-1} at room temperature.

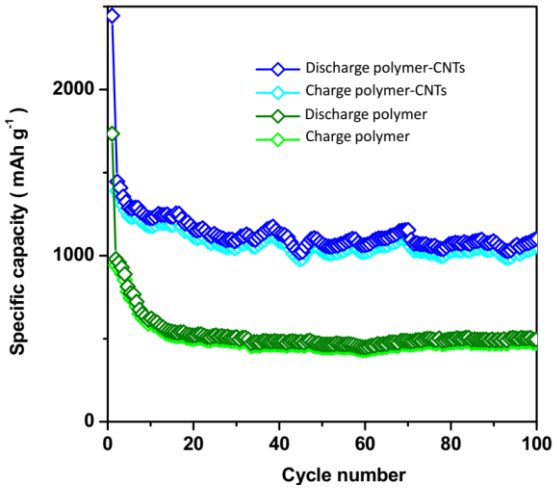

Figure 5. Charge-discharge cycle curves of (a) polymer and (b) polymer-CNTs nanofibers electrodes under current density of 0.05 A g^{-1} at room temperature.

Figure 5 shows the charge-discharge cycle graphs of pure polymer and polymer-CNT nanofiber electrodes at room temperature with a current density of 0.05 A g^{-1}. After 100 cycles, it is seen that the electrodes made of pure polymer and polymer-CNT nanofibers have reversible discharge capacities of 487.8 mAh g^{-1} and 1105.2mAh g^{-1}, respectively. The electrode made of polymer-CNT nanofibers shows no significant decay, indicating very good reversible capacity and cycling stability.

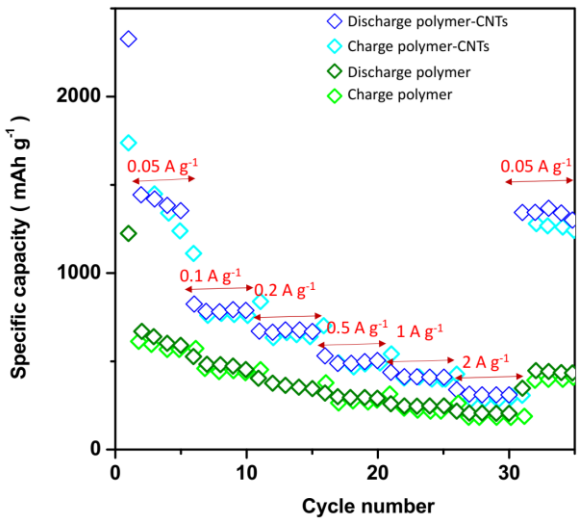

Figure 6. Results of study the rate performances of polymer and polymer-CNTs nanofibers electrodes under various current density from 0.05 A g^{-1} to 2 A g^{-1} at room temperature.

Figure 6 depicts the results of the study on the rate performances of both electrodes under various current densities from 0.05 A g^{-1} to 2 A g^{-1} at room temperature. As seen, the pure polymer nanofibers electrode obtains reversible capacity values at 0.05 A g^{-1} (760.1 mAh g^{-1}), 0.1 A g^{-1}

(487.2 mAh g^{-1}), 0.2 A g^{-1} (377.5 mAh g^{-1}), 0.5 A g^{-1} (291.5 mAh g^{-1}), 1 A g^{-1} (230.2 mAh g^{-1}), and 2 A g^{-1} (193.8 mAh g^{-1}) which are lower than that obtained reversible capacity values of polymer-CNTs nanofibers electrode at 0.05 A g^{-1} (1466.6 mAh g^{-1}), 0.1 A g^{-1} (848.5 mAh g^{-1}), 0.2 A g^{-1} (701.2 mAh g^{-1}), 0.5 A g^{-1} (539.3 mAh g^{-1}), 1 A g^{-1} (444.4 mAh g^{-1}), and 2 A g^{-1} (345.6 mAh g^{-1}). When the rate is tuned back to 0.05 A g^{-1} after cycling and cycling at different rates, the specific capacity of the polymer-CNTs nanofiber electrode can be recovered to 1374.5 mAh g^{-1}, which exhibits very stable cycling performance.

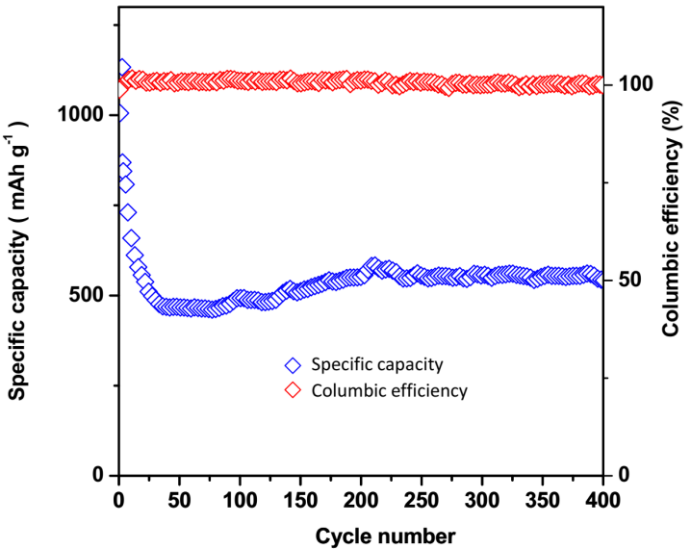

Figure 7. Results of study the long-term cycle performances and Columbic efficiency of polymer and polymer-CNTs nanofibers electrodes under current density of 0.2A g^{-1} in the voltage range of 0.001−3.0 V (vs Li/Li^+) at room temperature.

The findings of a study on the long-term cycle performances of polymer and polymer-CNT nanofiber electrodes at a current density of 0.2 A g^{-1} in the voltage range of 0.001–3.0 V (versus Li/Li^+) at ambient temperature are shown in Figure 7. As seen, over the first 25 cycles, the capacity is somewhat reduced. It may be connected to the development of unstable SEI coatings and the unchecked growth of Li dendrites, both of which led to unstable interfaces during repetitive Li plating and stripping, resulting in serious safety issues and a limited cycling life [68, 69]. The electrode made of polymer-CNT nanofibers, however, has a larger capacity and excellent cycle stability. According to studies, the as-prepared SEI made up of special nanotube arrays can effectively stop dendritic formation and prevent an unstable interface [68, 70]. Studies of the long-term cycle performances of polymer-CNT nanofiber electrodes reveal that after 400 cycles, a steady capacity of 598.8 mAh g^{-1} is attained. Therefore, it can be concluded that the addition of CNTs to the polymer-CNT nanofiber electrode exhibits greater rate capability and capacity than the electrode made entirely of polymer nanofibers. Table 1 compares the electrochemical performance of polymer-CNT nanofiber electrodes

with several reported carbon-based electrodes for lithium ion batteries, with polymer-CNT nanofiber electrodes showing higher or adequate performance.

Table 1. The comparison between the electrochemical performance of polymer-CNTs nanofibers electrode and various reported carbon based electrode for lithium ion batteries.

Materials	**Specific capacity (mAh g^{-1})**	**Cycle**	**Current density (mA g^{-1})**	**Ref.**
Carbon nanotubes grown on graphene paper	290	40	30	[71]
Derived carbon nanofiber webs	450	-	30	[72]
Hollow carbon nanofibers	501	10	50	[73]
Graphene nanosheets	834	15	50	[74]
Polyacrylonitrile/polypyrrole bicomponents-driven carbon nanofiber	454	50	50	[75]
Mesoporous carbon nanofibers	215	10	74.4	[76]
Graphene paper	~200	15	100	[77]
Carbon nanofibers	460	550	100	[78]
Activated carbon nanofibers	512	100	100	[79]
Nitrogen-doped graphene anchored on graphite foam	396	300	186	[80]
Polymer-CNTs nanofibers	1105.2	100	50	Present study
Polymer-CNTs nanofibers	598.8	400	200	Present study

4. CONCLUSION

The creation and investigation of carbon nanotube and polymer nanofibers as anodes for high-performance Li-ion batteries were the main goals of this effort. The process of electrospinning was utilized to create nanofibers made of polymer and CNTs. On the surface of the polymer-CNT nanofibers, structural studies showed the creation of many nanopores and a significant effective surface area. The electrochemical properties of the polymer-CNT nanofiber electrode were demonstrated to be highly reversible, and they demonstrated outstanding rate capabilities and strong cycling stability with a reversible capacity of 1105.2 mAh g^{-1} at a current density of 0.05 A g^{-1}. The polymer-CNT nanofiber electrode demonstrated a columbic efficiency of almost 100% and exhibited a steady and reversible capacity, according to the results. When compared to other published carbon-based electrodes for lithium-ion batteries, the electrochemical performance of polymer-CNT nanofiber electrodes was found to be superior or appropriate. As a result, the one-of-a-kind porous polymeric nanofibers can be used to improve the electrochemical performance of Li-ion batteries.

ACKNOWLEDGEMENT
The work is supported by the Fundamental Research Funds for the Central Universities, Theoretical Design and Performance Characterization of Sensitizers utilized in Nonmetal Dye-Sensitized Solar Cells (No. 31920160048).

References

1. H. Luo, C. Xu, B. Wang, F. Jin, L. Wang, T. Liu, Y. Zhou and D. Wang, *Electrochimica Acta*, 313 (2019) 10.

2. X. Zhang, Y. Tang, F. Zhang and C.S. Lee, *Advanced energy materials*, 6 (2016) 1502588.
3. W. Wang and Y.-C. Lu, *Accounts of Materials Research*, 2 (2021) 515.
4. X. Tong, F. Zhang, B. Ji, M. Sheng and Y. Tang, *Advanced Materials*, 28 (2016) 9979.
5. H. Maleh, M. Alizadeh, F. Karimi, M. Baghayeri, L. Fu, J. Rouhi, C. Karaman, O. Karaman and R. Boukherroub, *Chemosphere*, (2021) 132928.
6. B. Ji, F. Zhang, X. Song and Y. Tang, *Advanced materials*, 29 (2017) 1700519.
7. T. Gao, C. Li, Y. Wang, X. Liu, Q. An, H.N. Li, Y. Zhang, H. Cao, B. Liu and D. Wang, *Composite Structures*, 286 (2022) 115232.
8. R. Chen, X. Xue, Y. Hu, W. Kong, H. Lin, T. Chen and Z. Jin, *Nanoscale*, 11 (2019) 13282.
9. M. Wang, C. Jiang, S. Zhang, X. Song, Y. Tang and H.-M. Cheng, *Nature chemistry*, 10 (2018) 667.
10. T. Zhang, L. Zhang, L. Zhao, X. Huang, W. Li, T. Li, T. Shen, S. Sun and Y. Hou, *Small*, 16 (2020) 2005302.
11. S. Mu, Q. Liu, P. Kidkhunthod, X. Zhou, W. Wang and Y. Tang, *National science review*, 8 (2021) nwaa178.
12. T. Wei, Z.-M. Wang, Q. Zhang, Y. Zhou, C. Sun, M. Wang, Y. Liu, X.-Y. Qiu, S.-d. Xu and S. Qin, *CrystEngComm*, 24 (2022) 5014.
13. K. Liu, F. Ke, X. Huang, R. Yu, F. Lin, Y. Wu and D.W.K. Ng, *IEEE Transactions on Communications*, 69 (2021) 6675.
14. J. Fu, W. Kang, X. Guo, H. Wen, T. Zeng, R. Yuan and C. Zhang, *Journal of Energy Chemistry*, 47 (2020) 172.
15. T. Wei, Z. Wang, M. Zhang, Q. Zhang, J. Lu, Y. Zhou, C. Sun, Z. Yu, Y. Wang and M. Qiao, *Materials Today Communications*, 31 (2022) 103518.
16. Y. Shi, Z. Wang, L. Wen, S. Pei, K. Chen, H. Li, H.M. Cheng and F. Li, *Advanced Science*, 9 (2022) 2105419.
17. J. Dai, H. Feng, K. Shi, X. Ma, Y. Yan, L. Ye and Y. Xia, *Chemosphere*, 307 (2022) 135833.
18. Z.S. Iro, C. Subramani and S. Dash, *Int. J. Electrochem. Sci*, 11 (2016) 10628.
19. G. Li, H. Yuan, J. Mou, E. Dai, H. Zhang, Z. Li, Y. Zhao, Y. Dai and X. Zhang, *Composites Communications*, 29 (2022) 101043.
20. J. Liu, T. Li, H. Zhang, W. Zhao, L. Qu, S. Chen and S. Wu, *Materials Today Bio*, 14 (2022) 100243.
21. C. Zhao, M. Xi, J. Huo and C. He, *Physical Chemistry Chemical Physics*, 23 (2021) 23219.
22. H. Karimi-Maleh, R. Darabi, M. Shabani-Nooshabadi, M. Baghayeri, F. Karimi, J. Rouhi, M. Alizadeh, O. Karaman, Y. Vasseghian and C. Karaman, *Food and Chemical Toxicology*, 162 (2022) 112907.
23. C. Zhong, H. Li, Y. Zhou, Y. Lv, J. Chen and Y. Li, *International Journal of Electrical Power & Energy Systems*, 134 (2022) 107343.
24. D. Jia, Y. Zhang, C. Li, M. Yang, T. Gao, Z. Said and S. Sharma, *Tribology International*, 169 (2022) 107461.
25. Q.Z. Zhang, D. Zhang, Z.C. Miao, X.L. Zhang and S.L. Chou, *Small*, 14 (2018) 1702883.
26. H. Zhang, Y. Zhu, Z. Li, P. Fan, W. Ma and B. Xie, *Journal of Alloys and Compounds*, 744 (2018) 116.
27. H. Yang and S. Kou, *International Journal of Electrochemical Science*, 14 (2019) 7811.
28. J. Lv, Q. Huang, T. Liu and Q. Pan, *International Journal of Electrochemical Science*, 16 (2021) 210439.
29. G. Zheng, M. Chen, J. Yin, H. Zhang, X. Liang and J. Zhang, *International Journal of Electrochemical Science*, 14 (2019) 2345.
30. A.A. Almetwally, M. El-Sakhawy, M. Elshakankery and M. Kasem, *Journal of the Textile Association*, 78 (2017) 5.
31. R. Vasita and D.S. Katti, *International Journal of nanomedicine*, 1 (2006) 15.

32. H. Hou and D.H. Reneker, *Advanced Materials*, 16 (2004) 69.
33. R. Bhandavat and G. Singh, *The Journal of Physical Chemistry C*, 117 (2013) 11899.
34. J.-H. Chai and Q.-S. Wu, *Beilstein Journal of Nanotechnology*, 4 (2013) 189.
35. M. Yang, C. Li, Y. Zhang, Y. Wang, B. Li, D. Jia, Y. Hou and R. Li, *Applied Thermal Engineering*, 126 (2017) 525.
36. M. Wang, *Scientific reports*, 9 (2019) 1.
37. J. Kang, Y. Xue, J. Yang, Q. Hu, Q. Zhang, L. Gu, A. Selloni, L.-M. Liu and L. Guo, *Journal of the American Chemical Society*, 144 (2022) 8969.
38. H. Karimi-Maleh, C. Karaman, O. Karaman, F. Karimi, Y. Vasseghian, L. Fu, M. Baghayeri, J. Rouhi, P. Senthil Kumar and P.-L. Show, *Journal of Nanostructure in Chemistry*, (2022) 1.
39. P. Han, T. Yuan, L. Yao, Z. Han, J. Yang and S. Zheng, *Nanoscale research letters*, 11 (2016) 1.
40. F. Luna-Lama, D. Rodríguez-Padrón, A.R. Puente-Santiago, M.J. Muñoz-Batista, A. Caballero, A.M. Balu, A.A. Romero and R. Luque, *Journal of Cleaner Production*, 207 (2019) 411.
41. L. Huang, Q. Guan, J. Cheng, C. Li, W. Ni, Z. Wang, Y. Zhang and B. Wang, *Chemical Engineering Journal*, 334 (2018) 682.
42. T. Gao, Y. Zhang, C. Li, Y. Wang, Y. Chen, Q. An, S. Zhang, H.N. Li, H. Cao and H.M. Ali, *Frontiers of Mechanical Engineering*, 17 (2022) 1.
43. X. Li, Y. Chen, L. Zhou, Y.-W. Mai and H. Huang, *Journal of Materials Chemistry A*, 2 (2014) 3875.
44. Y. Xu, X. Chen, H. Zhang, F. Yang, L. Tong, Y. Yang, D. Yan, A. Yang, M. Yu and Z. Liu, *International Journal of Energy Research*, (2022) 1.
45. L. Yang, Q. Dai, L. Liu, D. Shao, K. Luo, S. Jamil, H. Liu, Z. Luo, B. Chang and X. Wang, *Ceramics International*, 46 (2020) 10917.
46. L. Tang, Y. Zhang, C. Li, Z. Zhou, X. Nie, Y. Chen, H. Cao, B. Liu, N. Zhang and Z. Said, *Chinese Journal of Mechanical Engineering*, 35 (2022) 1.
47. H. Karimi-Maleh, H. Beitollahi, P.S. Kumar, S. Tajik, P.M. Jahani, F. Karimi, C. Karaman, Y. Vasseghian, M. Baghayeri and J. Rouhi, *Food and Chemical Toxicology*, (2022) 112961.
48. L. Xia, S. Wang, G. Liu, L. Ding, D. Li, H. Wang and S. Qiao, *Small*, 12 (2016) 853.
49. Z. Savari, S. Soltanian, A. Noorbakhsh, A. Salimi, M. Najafi and P. Servati, *Sensors and Actuators B: Chemical*, 176 (2013) 335.
50. Y. Zhang, Q. Fu, Q. Xu, X. Yan, R. Zhang, Z. Guo, F. Du, Y. Wei, D. Zhang and G. Chen, *Nanoscale*, 7 (2015) 12215.
51. X. Wu, C. Li, Z. Zhou, X. Nie, Y. Chen, Y. Zhang, H. Cao, B. Liu, N. Zhang and Z. Said, *The International Journal of Advanced Manufacturing Technology*, 117 (2021) 2565.
52. A. Jaffe, A. Saldivar Valdes and H.I. Karunadasa, *Chemistry of Materials*, 27 (2015) 3568.
53. T. Gao, Y. Zhang, C. Li, Y. Wang, Q. An, B. Liu, Z. Said and S. Sharma, *Scientific reports*, 11 (2021) 1.
54. X. Wang, C. Li, Y. Zhang, H.M. Ali, S. Sharma, R. Li, M. Yang, Z. Said and X. Liu, *Tribology International*, 174 (2022) 107766.
55. N.I.T. Ramli, S.A. Rashid, M.S. Mamat, Y. Sulaiman, S.A. Zobir and S. Krishnan, *Electrochimica Acta*, 228 (2017) 259.
56. R. Savari, J. Rouhi, O. Fakhar, S. Kakooei, D. Pourzadeh, O. Jahanbakhsh and S. Shojaei, *Ceramics International*, 47 (2021) 31927.
57. H. Savaloni, E. Khani, R. Savari, F. Chahshouri and F. Placido, *Applied Physics A*, 127 (2021) 1.
58. W.J. Yu, L. Zhang, P.X. Hou, F. Li, C. Liu and H.M. Cheng, *Advanced Energy Materials*, 6 (2016) 1501755.
59. F. Chahshouri, H. Savaloni, E. Khani and R. Savari, *Journal of Micromechanics and Microengineering*, 30 (2020) 075001.

60. H. Savaloni, R. Savari and S. Abbasi, *Current Applied Physics*, 18 (2018) 869.
61. H. Xia, M. Lai and L. Lu, *Journal of Materials Chemistry*, 20 (2010) 6896.
62. Z. Said, S. Arora, S. Farooq, L.S. Sundar, C. Li and A. Allouhi, *Solar Energy Materials and Solar Cells*, 236 (2022) 111504.
63. Y. Chen, Z. Lu, L. Zhou, Y.-W. Mai and H. Huang, *Energy & environmental science*, 5 (2012) 7898.
64. X. Cui, C. Li, Y. Zhang, Z. Said, S. Debnath, S. Sharma, H.M. Ali, M. Yang, T. Gao and R. Li, *Journal of Manufacturing Processes*, 80 (2022) 273.
65. D. Luo, L. Zheng, Z. Zhang, M. Li, Z. Chen, R. Cui, Y. Shen, G. Li, R. Feng and S. Zhang, *Nature communications*, 12 (2021) 1.
66. Y. Jin, B. Zhu, Z. Lu, N. Liu and J. Zhu, *Advanced Energy Materials*, 7 (2017) 1700715.
67. C. Liu and J. Rouhi, *RSC Advances*, 11 (2021) 9933.
68. X. Li, S. Guo, H. Deng, K. Jiang, Y. Qiao, M. Ishida and H. Zhou, *Journal of Materials Chemistry A*, 6 (2018) 15517.
69. A.E. Anqi, C. Li, H.A. Dhahad, K. Sharma, E.-A. ATTIA, A. Abdelrahman, A.G. Mohammed, S. Alamri and A.A. Rajhi, *Journal of Energy Storage*, 52 (2022) 104906.
70. M. Yang, C. Li, Z. Said, Y. Zhang, R. Li, S. Debnath, H.M. Ali, T. Gao and Y. Long, *Journal of Manufacturing Processes*, 71 (2021) 501.
71. S. Li, Y. Luo, W. Lv, W. Yu, S. Wu, P. Hou, Q. Yang, Q. Meng, C. Liu and H.M. Cheng, *Advanced Energy Materials*, 1 (2011) 486.
72. C. Kim, K.S. Yang, M. Kojima, K. Yoshida, Y.J. Kim, Y.A. Kim and M. Endo, *Advanced Functional Materials*, 16 (2006) 2393.
73. B.-S. Lee, S.-B. Son, K.-M. Park, G. Lee, K.H. Oh, S.-H. Lee and W.-R. Yu, *ACS applied materials & interfaces*, 4 (2012) 6702.
74. D. Pan, S. Wang, B. Zhao, M. Wu, H. Zhang, Y. Wang and Z. Jiao, *Chemistry of Materials*, 21 (2009) 3136.
75. L. Ji, Y. Yao, O. Toprakci, Z. Lin, Y. Liang, Q. Shi, A.J. Medford, C.R. Millns and X. Zhang, *Journal of Power Sources*, 195 (2010) 2050.
76. P. Wang, D. Zhang, F. Ma, Y. Ou, Q.N. Chen, S. Xie and J. Li, *Nanoscale*, 4 (2012) 7199.
77. Y. Hu, X. Li, D. Geng, M. Cai, R. Li and X. Sun, *Electrochimica Acta*, 91 (2013) 227.
78. Y. Wu, M. Reddy, B. Chowdari and S. Ramakrishna, *ACS applied materials & interfaces*, 5 (2013) 12175.
79. C. Chen, R. Agrawal, Y. Hao and C. Wang, *ECS Journal of Solid State Science and Technology*, 2 (2013) M3074.
80. J. Ji, J. Liu, L. Lai, X. Zhao, Y. Zhen, J. Lin, Y. Zhu, H. Ji, L.L. Zhang and R.S. Ruoff, *Acs Nano*, 9 (2015) 8609.